Int J Clin Exp Med 2017;10(7):10091-10102
www.ijcem.com /ISSN:1940-5901/IJCEM0047359

*Original Article*

# Xanthohumol inhibits proliferation in lymphoma cells by generation of reactive oxygen species and G0/G1-phase cell cycle arrest

Fengling Min[1,2], Lina Zhang[1], Yongchun Chen[1], Lijia Zhai[1], Wei Zhou[1], Xiaohui Gao[1], Changjun Lin[2]

[1]*Department of Hematology, The Affiliated Hospital of Yangzhou University, Yangzhou University, The First People's Hospital of Yangzhou, Yangzhou 225001, China;* [2]*School of Life Sciences, Lanzhou University, Lanzhou 730000, China*

Received October 11, 2016; Accepted April 28, 2017; Epub July 15, 2017; Published July 30, 2017

**Abstract:** Xanthohumol (XN) exerts a broad spectrum of chemoprophylaxis actions. However, the mechanisms underlying effects of XN on lymphoma are still unclear. In this study, we used an apoptosis-resistant human Burkitt lymphoma cell line, Raji cells, in an in vitro model to assess the influence of XN on cell proliferation, DNA damage, and cell cycle progression, as well as the molecular mechanisms behind these processes. We found that Raji cell proliferation was inhibited significantly by XN at concentrations higher than 10 μM. This effect was dependent on both doses and times. Rapid accumulation of intracellular reactive oxygen species (ROS) in Raji cells was detected by DCFH-DA at 15 to 30 minutes post-exposure with XN. XN-treated cells exhibited DNA damage, which was related to ROS in Raji cells post-exposure with XN. Additionally, N-acetyl-L-cysteine (NAC) modestly decreased XN-induced cell death while XN caused G0/G1-phase cell cycle arrest in a manner unaffected by NAC exposure. Cell cycle arrest correlated with down-regulation of CDK4, cyclin E, phosphorylated cyclin E, and Cdc-2, but up-regulation of cyclin-dependent kinase inhibitor P21, all in a P53-independent manner. These results demonstrate that XN targets multiple signaling pathways to mediate ROS generation and cell cycle arrest, suggesting that XN may be a novel agent for treating lymphoma.

**Keywords:** Xanthohumol, lymphoma, ROS, cell cycle

## Introduction

During the last decade, treatment outcomes of lymphomas have improved considerably with the introduction of monoclonal antibodies, Bruton's tyrosine kinase inhibitors, and immunomodulatory drugs [1]. However, traditional combination chemotherapy is still the standard treatment for aggressive Non-Hodgkin's lymphomas (NHL). Burkitt lymphoma, an aggressive form of B-cell NHL, commonly occurs in children and young adults. A characteristic of Burkitt lymphoma is rapid cell proliferation due to constitutive overexpression and constant activation of c-Myc, an oncogenic protein, via chromosomal translocation (8;14) (q24;q32) [2]. Although intensive chemotherapy has improved treatment outcomes, some patients eventually relapse due to drug resistance. Thus, continued efforts to seek new drugs for improving chemotherapeutic efficacy are needed.

More than 70% of all drugs currently used for cancer therapies are derived from natural sources. XN, a major prenylated chalcone from hops (*Humulus lupulus* L.), has received much attention recently due to its multiple pharmacological activities, including anti-proliferative, anti-inflammatory, antioxidant, pro-apoptotic, anti-bacterial, and anti-adhesive effects [3]. Several studies have shown that XN inhibits the growth of cancer cells in various organs, including the larynx, breast, pancreas, colon, liver, and blood, among others [4-6]. However, little is known about the biological effects of XN on lymphoma cells. The mechanisms of growth inhibition by XN vary, depending on the type of cancer cells. XN could be particularly active during the aggressive phases of the disease.

Drug-resistant cancer cells are hypersensitive to XN [6]. XN does not affect drug-resistance, but instead, causes a sort of drug adaptation, which is characterized by downregulation of FAK, AKT and NF-κB activities, rendering cells less invasive and more susceptible to cytotoxic drugs [6-8]. Aberrant NF-κB activation, with increased expression of pro-proliferative and anti-apoptotic genes, is a characteristic of drug-resistant lymphoid tumors [9]. These data collectively prompted us to investigate whether XN might be a potential therapeutic option for the treatment of aggressive lymphoma. EBV-infected Raji cells, a human Burkitt lymphoma cell line, have been resistant to apoptosis due to defects other than p53 mutation, such as impaired apoptotic signal transduction in the cytoplasm [10]. In this study, we used Raji cells as an *in vitro* model to investigate the influence of XN on cell proliferation, ROS generation, and cell cycle disruption. Additionally, the molecular mechanisms behind these processes were analyzed.

## Materials and methods

### *Cell culture and reagents*

Raji cells, an EBV-infected human Burkitt's lymphoma cell line, were obtained from the Cell Bank of the Chinese Academy of Sciences (Shanghai, China). Raji cells were cultured in RPMI-1640 medium (Gibco) supplemented with 10% heat-inactivated fetal bovine serum (Si-Ji-Qing Biotechnology, Hangzhou, China), 100 U/ml penicillin and 100 mg/ml streptomycin. XN and the cell permeable ROS scavenger, NAC, were purchased from Sigma-Aldrich (St. Louis, MO, USA). 2',7'-Dichlorofluorescein diacetate (DCFH-DA) was obtained from Beyotime. DCFH-DA was dissolved in DMSO to a working concentration of 20 mM before use. Anti-γ-H2AX and anti-phosphorylated histone H2AX (Ser 139) mouse monoclonal antibodies (Upstate Biotechnology, Inc., NY) were purchased from Invitrogen. Anti-β-actin antibodies were purchased from Sigma Chemical Co. (St. Louis, MO, USA). The antibodies against Cdc-2, CDK4, phosphorylated cyclin E (Thr160), cyclin E, phosphorylated P53 (Ser15), P53, and P21, as well as the horseradish peroxidase (HRP)-labeled goat anti-mouse or anti-rabbit IgG antibodies were purchased from Cell Signaling Technology (Beverly, MA). Paraformaldehyde was obtained from Fluka Co., USA.

### *Sulforhodamine B protein biomass assay*

Raji cells were incubated in 96-well plates in the presence of increasing concentrations of XN, which were added at different times. Cell growth was measured using the sulforhodamine B (SRB)-staining assay for whole culture protein determination. Briefly, after completion of incubation, Raji cells were fixed with cold trichloroacetic acid (TAC) for 1 h. Moreover, 100 μl SRB solution was added to each well and cultured for 10 min. Unbound SRB was washed five times with 1% acetic acid, followed by air drying. The bond stain was solubilized with Tris buffer, and the absorbance of the liberated dye was assayed at a single wavelength of 515 nm.

### *Determination of cell death*

Cell death was quantified using a rapid propidium iodide (PI) inclusion assay. Briefly, cell pellets were resuspended in PI staining buffer, supplemented with RNase (100 μg/mL). Cells were stained for 15 minutes at room temperature in the dark. Samples were kept on ice and then analyzed by flow cytometry.

### *Measurement of reactive oxygen species*

Intracellular accumulation of ROS was determined using DCFH-DA. NAC was used as a ROS scavenger and was added to the culture medium 1 h before XN treatment. Raji cells were treated with XN, in the absence or presence of NAC at 5 mM, for various periods of time. Cells were washed with PBS and then incubated in the presence of 10 μM DCFH-DA in PBS for 30 min at 37°C in the dark. Cells were then collected by centrifugation and washed with PBS. Fluorescence was determined by flow cytometry with Win-MDI software at an excitation filter of 480 nm and an emission filter of 525 nm.

### *Immunofluorescence*

An γ-H2AX antibody was used to visualize breaks within double-stranded DNA (dsDNA) using methods described previously [11]. Cells were pretreated with or without NAC for 1 h. Then, the cells were exposed to 20 μM XN and incubated for various times to characterize the extent of the different treatment-induced DNA double-strand breaks. After various treatment times, cells were fixed with 4% paraformaldehyde, and then permeabilized with Triton X-100

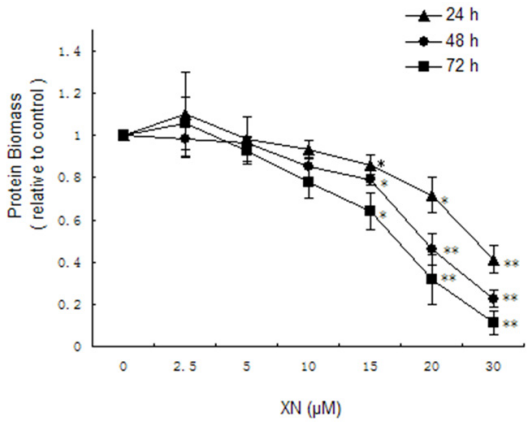


**Figure 1.** Effect of XN on cell protein biomass in Raji cells. Cells were treated with various concentrations of XN for the indicated time periods. Cell protein biomass (relative to controls) was determined by SRB staining. The data are presented as the means ± SEM. Error bars represent the SEM of 3 independent experiments.

in a 1% (w/v) solution of bovine serum albumin. After permeabilization, the cells were incubated with a primary antibody against γ-H2AX at a dilution of 1:2000 for 2 h at 37°C, then washed twice with PBS and resuspended in 100 μl of a 1:2000 diluted solution of secondary antibody, which was conjugated to fluorescein isothiocyanate (FITC), for 30 min at room temperature in the dark. Images were acquired using confocal microscopy with a 100× objective. Untreated cells were also examined for γ-H2AX foci using the same time course as the controls. A minimum of 100 cells was counted for each treatment.

*Alkaline comet assay*

Cells were treated with 20 μM XN for different lengths of time in the absence or presence of NAC at 5 mM. Samples were collected at different time points and processed for comet assay. Briefly, cell suspensions were adjusted to $10^5$ cells/ml in ice-cold PBS and mixed with LMAgarose for immediate loading onto regular agarose pre-coated slides. The third layer, with an equal volume of LMAgarose gel, was then loaded onto the solidified second gel and cooled with ice. The slides were incubated for 1 h at 4°C in lysis solution, and then immersed in freshly prepared alkaline electrophoresis buffer for 30 minutes at 4°C in the dark. Electrophoresis was carried out for 30 min at 20 V in electrophoresis solution. Cells were stained with ethidium bromide and analyzed with a fluorescence microscope (Zeiss Axioplan 2) equipped with a Hamamatsu Orca-EC camera. Tail moment of 50-100 randomly selected cells was measured using OpenComet software.

*Cell cycle analysis*

Cell cycle distribution was analyzed using flow cytometric measurement of the DNA content of the cells. Cells were treated with 20 μM XN for 24 or 48 h. All cells were harvested, fixed in 3 ml 95% ice-cold ethanol. Prior to flow cytometry, the cells were stained at 4°C for 3 h in PBS containing Triton X-100, PI, and RNase A. The cells were incubated for 15 min at room temperature in the dark, and the DNA content of the cells was analyzed using a FACScan instrument (Becton Dickinson, San Jose, CA).

*Western blot analysis*

Raji cells were treated with 20 μM XN for 36 h. After treatment, cells were washed with ice-cold PBS, and then lysed in ice-cold lysis buffer for 30 min. Cell lysates were centrifuged at 12000 rpm for 10 min at 4°C and protein concentrations in supernatants were determined using the Bio-Rad protein assay kit. Proteins (40 μg) were electrophoresed on 5-13.5% polyacrylamide gels. The gels were transferred onto nitrocellulose membranes that were incubated with relevant antibodies. The following antibodies were used: Phospho-P53 (Ser15), P53, P21, Phospho-cyclin E (Thr160), cyclin E, Cdc-2, CDK4 (at a dilution of 1:1000), and β-actin (at a dilution of 1:5000). Then, membranes were washed three times with TBST for 5 min each, and incubated with HRP-labeled mouse or rabbit IgG antibodies for 1 h at room temperature. The signals of detected proteins were visualized on an ECL plus system (Amersham Pharmacia Biotech). *β*-actin expression was used as reference band.

*Data analysis*

Group differences were examined using analysis of variance (ANOVA) and independent samples t-test. Differences were considered significant at $P < 0.05$. The asterisks displayed on the figures represent the degree of statistical significance as determined by *P* values as follows: * < 0.05, ** < 0.01. All of the analyses were

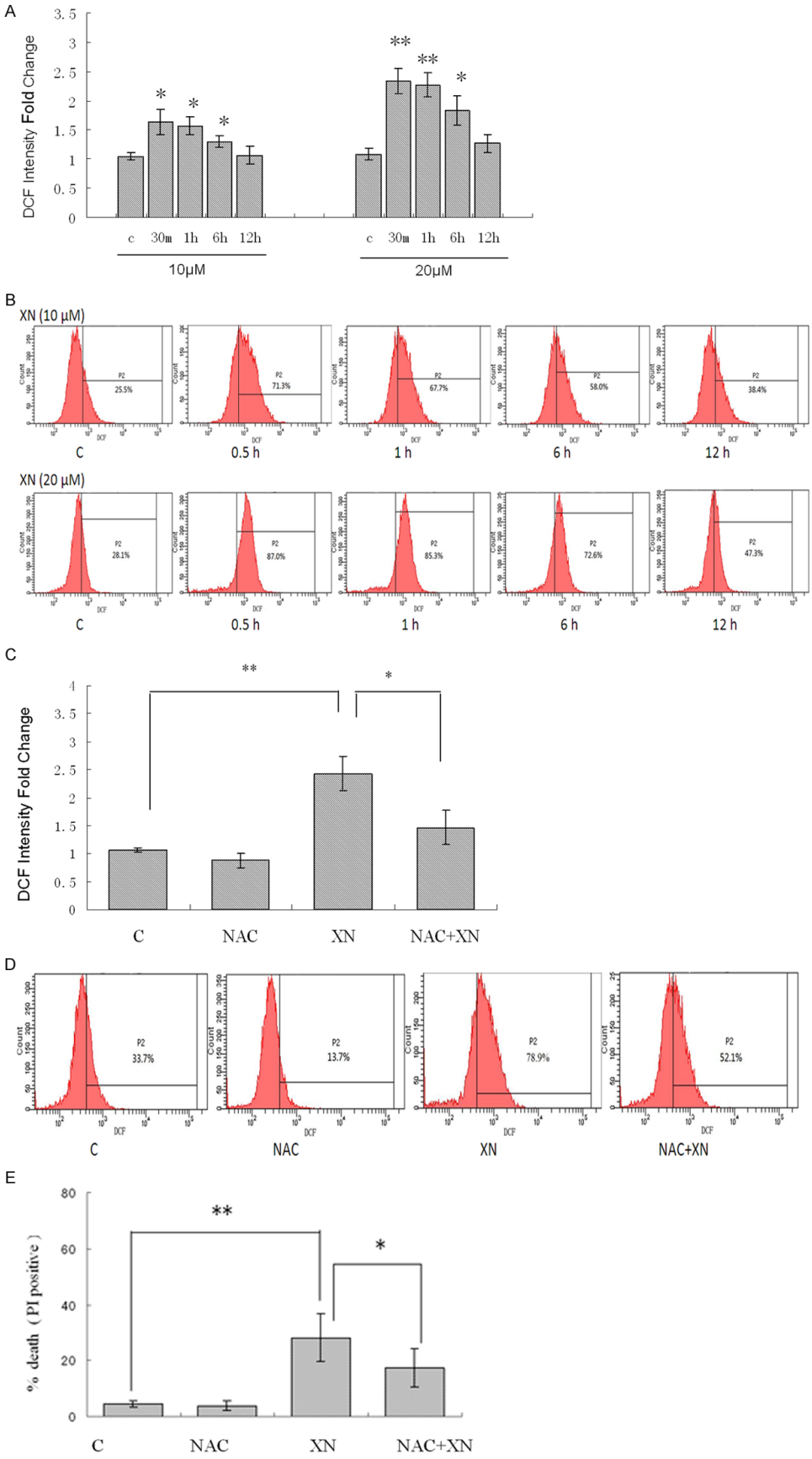
A
DCF Intensity Fold Change
c 30m 1h 6h 12h
10μM
20μM
B
XN (10 μM)
XN (20 μM)
C
0.5 h
1 h
6 h
12 h
C
DCF Intensity Fold Change
C
NAC
XN
NAC+XN
D
C
NAC
XN
NAC+XN
E
% death (PI positive)
C
NAC
XN
NAC+XN

**Figure 2.** XN induces ROS production in Raji cells. The antioxidant NAC inhibits XN-induced cytotoxicity. (A) Cells were treated with 10 μM and 20 μM XN, then stained with H2DCFDA to assess intracellular ROS levels at indicated time points. (B) Representative images of ROS generation by flow cytometry using DCFH-DA. (C and D) Before adding 20 μM XN, cells were treated with 5 mM NAC for 1 h or treated with XN alone. ROS production was then determined 30 min later using H2DCFDA staining, and analyzed by flow cytometry. (E) Cells were treated with 20 μM XN alone or pretreated for 1 h with NAC, and the amount of XN-induced cell death was quantified at 24 h using PI staining as described in "Materials and Methods". The control cells (C) were the untreated group. The data are presented as the means ± SD. Experiments were performed in triplicate and repeated twice.

performed using the SPSS17.0 (Statistical Package for the Social Sciences) software.

## Results

*XN decreases protein biomass in Raji cells*

The SRB assay of cell protein biomass was performed after 24 h, 48 h and 72 h exposure to XN treatment at increasing concentrations of XN, as showed in **Figure 1**. Raji cell proliferation was not affected by 2.5 μM or 5 μM within 72 h exposure period. Similar treatment exposures using 15 μM or higher concentration XN significantly reduced cell proliferation at 24 h ($P < 0.05$). Under these conditions, normal immortalized human lymphoblastoid cell line is more resistant to XN (data not shown). XN significantly inhibited proliferation of Raji cells with IC50 values of 27.8 μM, 19.4 μM and 16.2 μM at 24 h, 48 h and 72 h, respectively. Inhibition of cell proliferation was dependent on both dose and time (**Figure 1**). Based on these results, all subsequent studies were conducted at an XN concentration of 20 μM.

*XN induced intracellular ROS in Raji cells*

To investigate potential mechanisms of inhibition of Raji cell proliferation by XN treatment, we measured the kinetics of total ROS generation by flow cytometry using DCFH-DA. Addition of 5 mM NAC did not affect intracellular ROS in Raji cells. As seen in **Figure 2A** and **2B**, maximum levels of intracellular ROS were observed at 15 to 30 minutes after initial exposure to XN. Peak ROS production lasted 1-2 h, followed by a gradual decline to base level at 12 h. However, pre-treatment with the ROS scavenger, NAC (5 mM), for 1 h, significantly inhibited intracellular ROS production (**Figure 2C** and **2D**). To determine whether XN-induced inhibition of cell proliferation and ROS generation correlated with cell death, a PI assay was used in conjunction with flow cytometry. Addition of NAC (5 mM) alone caused a marginal effect in the level of basal cell viability. Raji cells were pre-treated with NAC, and then treated with 20 μM XN for 24 h. The death rates of cells treated with XN alone decreased from 28.2% to 17.5% when treated with XN in the presence of NAC. These results indicate that NAC significantly inhibited XN induced cell death. However, inhibition was not complete, as some level of cell death was still observed (**Figure 2E**). Accordingly, these data suggest that production of ROS contributes to cell death caused by XN treatment.

*XN causes DNA damage in Raji cells*

ROS damage a variety of biomolecules: proteins, RNA, and DNA. Many stimuli, such as tumor necrosis factor, anticancer drugs, and chemopreventive agents, stimulate cells to produce ROS, which subsequently activates cell death machinery. To find if XN treatment of Raji cells causes DNA damage, DNA double strand breaks (DSB) were measured relative to γ-H2AX expression. An early cellular response to DSBs is the phosphorylation at Ser139 of H2AX (γ-H2AX), a subclass of eukaryotic histones that are part of the chromatin structure. Less than 20% cells showed 1 to 5 γ-H2AX foci in untreated Raji cells. In contrast, the number of cells with γ-H2AX foci was dramatically increased after exposure to 20 μM XN. Pretreatment with NAC (5 mM) for 1 h caused the DNA DSB damage to be completely restored (**Figure 3A**). Thirty minutes after XN treatment, the percentage of cells with γ-H2AX foci increased to 78.1% compared with 22.9% in controls, a result with significant statistical difference. The formation of γ-H2AX foci in cells gradually disappeared at 4 h after XN treatment (**Figure 3B**). Importantly, no cell death was observed until the first 12 h after 20 μM XN exposure. Thus, the formation of DSB was not a secondary event due to internucleosomal DNA cleavage in the apoptotic process.

Because phosphorylation of H2AX induces activation of repair machinery rapidly, phosphoryla-

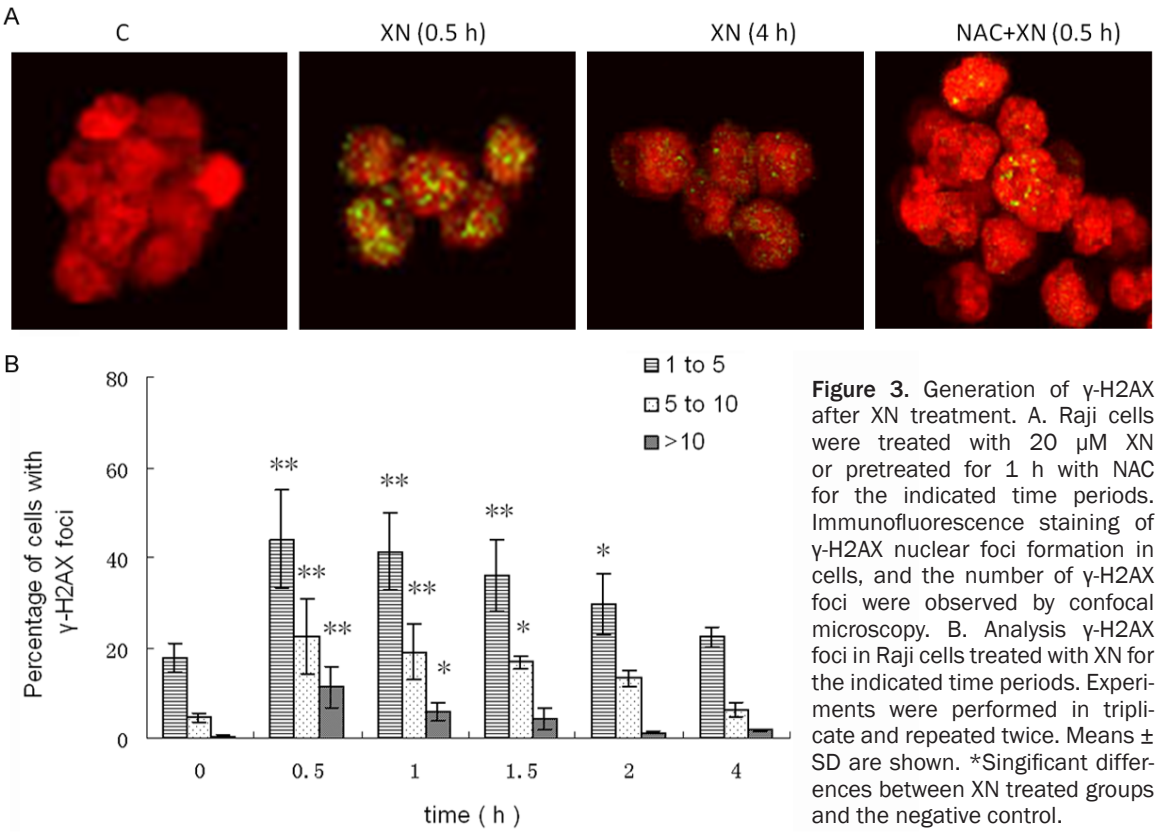


**Figure 3.** Generation of γ-H2AX after XN treatment. A. Raji cells were treated with 20 μM XN or pretreated for 1 h with NAC for the indicated time periods. Immunofluorescence staining of γ-H2AX nuclear foci formation in cells, and the number of γ-H2AX foci were observed by confocal microscopy. B. Analysis γ-H2AX foci in Raji cells treated with XN for the indicated time periods. Experiments were performed in triplicate and repeated twice. Means ± SD are shown. *Singificant differences between XN treated groups and the negative control.

tion does not reflect true DNA breaks. To further verify DNA breaks, we performed single cell gel-electrophoresis (alkaline comet assay), which is a more powerful and direct assay for the detection of DNA breaks. Our results revealed that XN could significantly increase the tail moment of Raji cells at 30 min after XN exposure. However, as time went on, the tail moment decreased, until no difference was observed compared with untreated Raji cells 6 h later. Pre-treatment with 5 mM NAC for 1 h significantly restored DNA damage (**Figure 4A** and **4B**). These results indicate that NAC, an antioxidant, diminishes the DNA-damaging effects of XN in Raji cells, which confirms that XN damages DNA through oxidative stress.

*XN induces G0/G1 cell cycle arrest*

As shown in **Figure 5**, after 24 h treatment with 20 μM XN, the percentage of G0/G1 cells significantly increased from 45.79% (control) to 66.48% ($P < 0.05$). This arrest in G0/G1 phase was accompanied by a concomitant decrease in S phase cells. The increased accumulation of cells in G0/G1 phase was sustained after 48 h treatment with 20 μM XN. In addition, pre-treatment with NAC at 5 mM for 1 h resulted in a slight reduction in the percentage of cells in the G0/G1 phase, a finding that was not significantly different from that of Raji cells treated with XN alone.

*Expression of cell cycle regulator proteins after XN treatment*

To characterize the molecular mechanism of XN induced G0/G1 cell cycle arrest in Raji cells, we investigated the expression patterns of cell cycle regulatory proteins that are responsible for G0/G1 cell cycle regulation using western blot analysis. As shown in **Figure 6**, XN treatment caused a significant decrease in the expression of cyclin E, phosphorylated cyclin E, and CDK4 in a time-dependent manner. Cdc-2 protein is present in a moderate amount within 8 h in cells treated with XN, and then decreases dramatically 12 h post-treatment. Cdc-2 was barely detectable 16 h later in cells treated with XN. Although the effect of XN treatment on the levels of P53 and phosphorylated P53 was not determined in this study, a marked XN mediated induction of P21 was observed. These results demonstrate that cyclins-CDK-CDKI

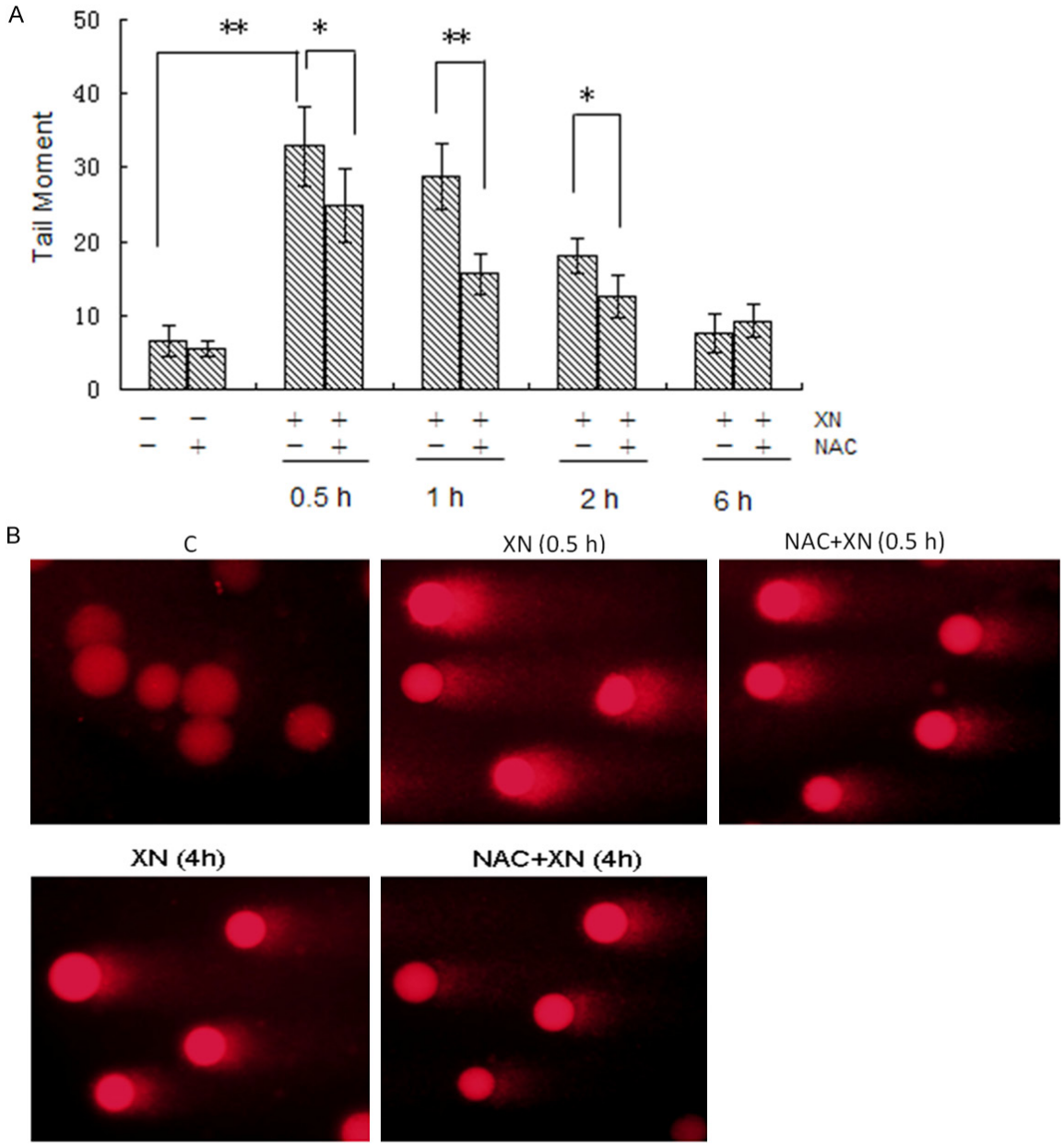


**Figure 4.** Analysis of XN induced DNA damages by comet assay. Raji cells were treated with 20 μM XN alone or pretreated for 1 h with NAC, DNA damage was assessed at indicated time point. A. The level of DNA strand breaks are expressed as the tail moment in the comet tails, and 50 to 100 comets were analyzed per experimental point in each of three independent experimental cultures. The data are presented as the means± SD. B. Representative images of DNA strand breaks.

may play an important role in XN-induced G0/G1 cell cycle arrest, activation of P21 and attenuation of Cdc-2 independent of P53 status in Raji cells.

## Discussion

XN is the most abundant prenylated flavonoid in hops, a common ingredient of beer. The structure of XN was first identified by Verzele in 1957, but only in the last decade has XN been found to exhibit a broad spectrum of biological properties, including anti-cancer activity [12]. XN by itself was not cytotoxic to Raji cells at low concentrations, and showed a significant protective effect against DNA damage caused by pro-carcinogens and ROS-inducing agents. However, at high concentrations, XN has signifi-

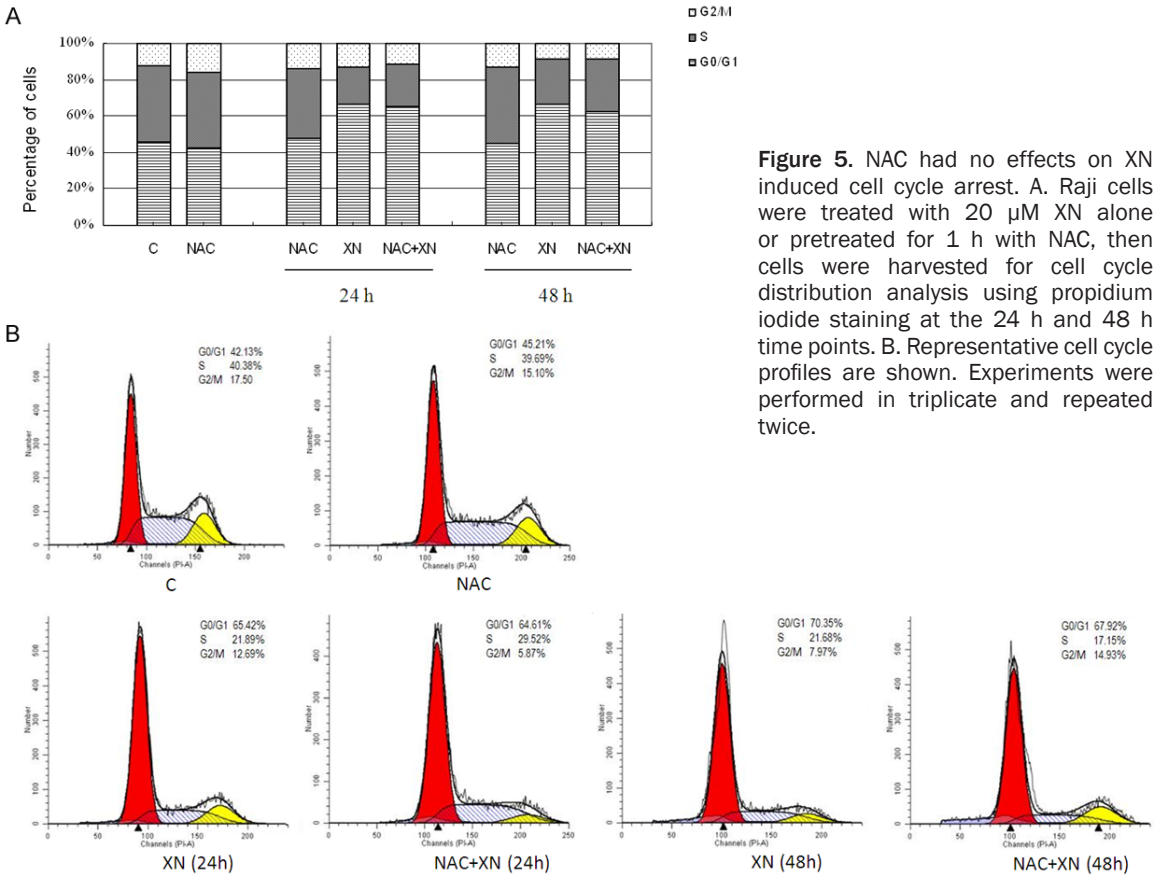


**Figure 5.** NAC had no effects on XN induced cell cycle arrest. A. Raji cells were treated with 20 μM XN alone or pretreated for 1 h with NAC, then cells were harvested for cell cycle distribution analysis using propidium iodide staining at the 24 h and 48 h time points. B. Representative cell cycle profiles are shown. Experiments were performed in triplicate and repeated twice.

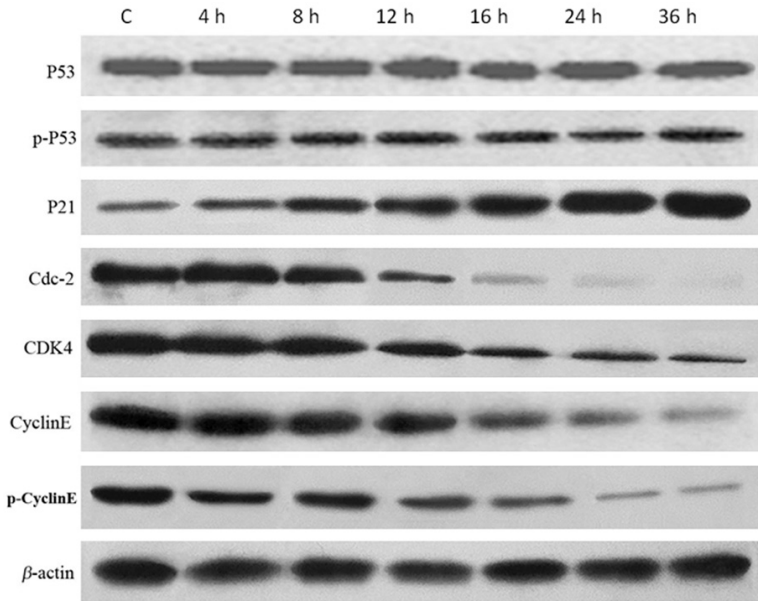


**Figure 6.** Western blot analysis of cell cycle regulatory protein after treatment with XN on Raji cells. Cells were treated with 20 μM XN for indicated time periods and the cell lysates were prepared as described in "Materials and Methods". Cell extracts were subjected to western blot analysis for determining the expression of human P53, phosphorylated P53, P21, Cdc-2, CDK4, cyclin E, and phosphorylated cyclin E. β-actin was used as a loading control. A representative result from three independent experiments is shown.

cant anti-cancer activity *in vitro* and *in vivo*. Cells derived from normal tissue are less prone to the cytotoxic effects of XN. XN does not inhibit growth of bone marrow progenitors isolated from healthy volunteers [8]. At concentrations up to 100 μM, XN does not affect the growth of human hepatocytes or endothelial cells [13, 14]. The differential cytotoxic response between normal and tumor cells suggests that XN may be a potential candidate as a cancer chemotherapeutic drug. In this study, XN at concentrations higher than 15 μM significantly reduced proliferation of EBV-infected Raji cells at 24 h post-treatment. However, normal immortalized human lymphoblastoid cell line without tumor features preserve the genetic characteristics of lymphocyte B donor, which possess are

resistant to XN (data not shown). The antiproliferative effect of XN on Raji cells was dependent on both dose and time. These data indicate that the mechanisms behind the antitumor effect of XN are associated with the change of molecular biologic characteristics in cells from normal to tumor development.

ROS generation induced by XN treatment may be a feature shared with other cancer cells because it has been observed in other cancer cells [7, 15]. Patterns of ROS induction vary in cells of different tissue origins. XN induces transient ROS formation in benign prostate hyperplasia cells. Even the transient induction of superoxide anion radical triggers antiproliferative activity and apoptosis [3]. Prostate cancer cells and human chronic myelogenous leukemia cells produce strong and continuous ROS after XN treatment, though the time to a maximum level and the time of duration are different [7, 15]. In this study, in Raji cells, ROS content in response to XN rapidly reached a maximum level following 15-30 min of treatment and then declined at 12 h. The duration of this treatment is shorter than that of the other reports in the literature. These data indicate that cancer cells from different tissues have respond differently to XN treatment with respect to ROS.

The neutral comet assay detects DNA double strand breaks (DSBs) exclusively, whereas the alkaline comet assay detects both DNA double and single strand breaks, in addition to alkali-labile sites. As previously reported, 50-75 breaks per cell could be the comet assay detection limit [16]. To increase detection sensitivity, we used the alkaline comet assay to detect DNA breaks. Here we show that XN significantly increases the tail moment of Raji cells after XN exposure. However, both tail moment and production of γ-H2AX foci decreased dramatically overtime, which suggests a strong, quick, and efficient repair of damaged DNA in Raji cells. EBV-infected Raji cells, as well as other EBV-positive cell lines, have efficient DNA damage repairing systems. Up to 59% of DNA double-strand breaks in Raji cells caused by radiation are repaired within 1 h [17]. Furthermore, along with γ-H2AX foci formation in nuclei as described above, pre-treatment with NAC for 1 h significantly decreased XN induced DNA damage, with respect to both tail moment and production of γ-H2AX foci. These results indicate that NAC, a ROS scavenger, diminishes the DNA-damaging effects of XN in Raji cells, which confirms that XN damages DNA through oxidative stress. In accordance with previous reports [7], we found that cell death caused by 20 μM XN treatment was partly abrogated in the presence of NAC, which further supports the concept of ROS partly participating in XN induced Raji cell growth inhibition.

In this study, Raji cells treated with XN for 24 h were arrested in G0/G1 cell cycle phase, a response that was sustained to 48 h. NAC pretreatment had no effect on cell cycle arrest after XN treatment, which suggests that the generation of ROS may not affect cell cycle arrest induced by XN. Whether the phenomenon might be ascribed to short duration of ROS production or quick and efficient repairing of damaged DNA in Raji cells is not clear. The induction of cell cycle arrest by XN has been reported in other cellular models, but the involved mechanisms may be dependent on the cell line used [3, 4, 18]. The cell cycle is considered to be a major regulatory mechanism for cell growth. Cell cycle progression is regulated by a sequential activation of cyclin dependent kinases (CDK). Cyclin D and cyclin E, together with CDK2, CDK4, or CDK6, play important roles in the progression of cells through the G0/G1 phase of the cell cycle [19]. Overexpression of cyclins and CDKS can provide cancer cells with growth advantage [20]. On the other hand, CDK inhibitors (CDKI) are considered tumor suppressors and negatively regulate cell cycle progression by binding the inhibiting kinase activities of CDKS/cyclins. Therefore, some molecule inhibitors that target cyclin/CDK complexes have been discovered as an effective strategy for cancer treatment [21]. Tumor suppressor P53 regulates the G0/G1 and G2/M phase of the cell cycle, resulting in growth arrest. Previous reports have found that P21, the target of P53, is one of the major CDKI that directly inhibit the activity of CDKs, thereby leading to cell cycle arrest in G1 phase [22]. It is generally believed that P21 expression is rarely P53-independent because its expression is hindered in cells with p53 knockout [23]. However, P53-independent P21 expression has been observed in p53 wild type and p53 null carcinoma cells [24]. Even the Raji cells have p53 mutants, and mutated proteins

could be stabilized in these cells and thereby accumulate to relatively high levels [25]. In our experiments, XN increased the percentage of G0/G1 cells by significant decrease in the expression of CDK4 and cyclin E, and phosphorylation of cyclin E, but had no effect on accumulation or activation of P53. Strong levels of P21 were induced 8 h later in cells treated with XN. Although the activation of p21 is mainly regulated by the activation of tumor suppressor protein P53 [26], our results indicate that activation of P21 does not necessarily require P53. Because P21 expression is also regulated by other P53 family proteins (e.g., P73 and P63), it is possible that these proteins contribute to P21-mediated G0/G1 arrest by XN [27].

Cdc-2, or cyclin-dependent kinase 1, plays a role in regulating the G2/M transition, but its synthesis begins at the late G1 to S of the cycle. Cdc-2 also operates in G1 phase and is involved in the commitment of cells into the proliferative cycle [28]. Cdc-2 is a cell growth activating protein, and inhibition of Cdc-2 is associated with cell growth inhibition. Previous studies suggest that P53 may suppress the Cdc-2 promoter through induction of P21 [29]. In Raji cells, an abnormal cell cycle regulatory networkcould be responsible for the transformed phenotype of malignancy [30]. Our data show that Cdc-2 protein levels decreased dramatically in amount 12 h after XN treatment to a barely detectable level 16 h later. Over-expressed Cdc-2 phosphorylating survive has been found to be one of the causes of paclitaxel-resistant ovarian cancer [31]. Knockdown of Cdc-2 expression might suppress the malignant phenotype and overcoming Cdc-2-associated chemoresistance in patients with malignant glioma [32]. XN could be particularly active during the aggressive phases of the disease [6]. Drug resistant cancer cells still remain hypersensitive to XN [7]. In the present study, attenuating Cdc-2 expression by XN, independent of P53 status, suppressed Raji cell growth, suggesting that Cdc-2 may be a potential target for treatment of EBV-infected lymphoma characterized by rapid growth and drug-resistance.

In conclusion, our results demonstrate that XN induces ROS generation and ROS-mediated DNA damage in Raji cells. XN inhibits the proliferation of Raji cells by inducing G0/G1 cell cycle arrest through up-regulating the expression of P21 and down-regulating the expression of Cyclin E, phosphorylated cyclin E, CDK4, and Cdc-2 in a P53-independent manner. Involvement of multiple signaling pathways targeted by XN in mediating DNA damage and cell cycle arrest in Raji cells suggests that XN might be a novel agent for the management of rapid growth and drug-resistant lymphoma.

## Disclosure of conflict of interest

None.

**Address correspondence to:** Dr. Fengling Min, Department of Hematology, The Affiliated Hospital of Yangzhou University, Yangzhou University, The First People's Hospital of Yangzhou, Yangzhou 225001, China. Tel: +86-15952781935; E-mail: 1014121694@qq.com (FLM); Changjun Lin, School of Life Sciences, Lanzhou University, Lanzhou 730000, China. Tel: +86-15117160343; E-mail: linc@lzu.edu.cn (CJL)

## References

[1] Arita A, McFarland DC, Myklebust JH, Parekh S, Petersen B, Gabrilove J and Brody JD. Signaling pathways in lymphoma: pathogenesis and therapeutic targets. Future Oncol 2013; 9: 1549-1571.

[2] Said J, Lones M and Yea S. Burkitt lymphoma and MYC: what else is new? Adv Anat Pathol 2014; 21: 160-165.

[3] Strathmann J, Klimo K, Sauer SW, Okun JG, Prehn JH and Gerhauser C. Xanthohumol-induced transient superoxide anion radical formation triggers cancer cells into apoptosis via a mitochondria-mediated mechanism. FASEB J 2010; 24: 2938-2950.

[4] Slawinska-Brych A, Krol SK, Dmoszynska-Graniczka M, Zdzisinska B, Stepulak A and Gagos M. Xanthohumol inhibits cell cycle progression and proliferation of larynx cancer cells in vitro. Chem Biol Interact 2015; 240: 110-118.

[5] Wang Y, Chen Y, Wang J, Chen J, Aggarwal BB, Pang X and Liu M. Xanthohumol, a prenylated chalcone derived from hops, suppresses cancer cell invasion through inhibiting the expression of CXCR4 chemokine receptor. Curr Mol Med 2012; 12: 153-162.

[6] Dell'Eva R, Ambrosini C, Vannini N, Piaggio G, Albini A and Ferrari N. AKT/NF-kappaB inhibitor xanthohumol targets cell growth and angiogenesis in hematologic malignancies. Cancer 2007; 110: 2007-2011.

[7] Benelli R, Vene R, Ciarlo M, Carlone S, Barbieri O and Ferrari N. The AKT/NF-kappaB inhibitor xanthohumol is a potent anti-lymphocytic leu-

kemia drug overcoming chemoresistance and cell infiltration. Biochem Pharmacol 2012; 83: 1634-1642.
[8] Monteghirfo S, Tosetti F, Ambrosini C, Stigliani S, Pozzi S, Frassoni F, Fassina G, Soverini S, Albini A and Ferrari N. Antileukemia effects of xanthohumol in Bcr/Abl-transformed cells involve nuclear factor-kappaB and p53 modulation. Mol Cancer Ther 2008; 7: 2692-2702.
[9] Liu X, Wang B, Ma X and Guo Y. NF-kappaB activation through the alternative pathway correlates with chemoresistance and poor survival in extranodal NK/T-cell lymphoma, nasal type. Jpn J Clin Oncol 2009; 39: 418-424.
[10] Kawabata Y, Hirokawa M, Kitabayashi A, Horiuchi T, Kuroki J and Miura AB. Defective apoptotic signal transduction pathway downstream of caspase-3 in human B-lymphoma cells: a novel mechanism of nuclear apoptosis resistance. Blood 1999; 94: 3523-3530.
[11] Fengling M, Qingxiang G, Lijia Z and Wei Z. Influx of extracellular calcium participates in rituximab-enhanced ionizing radiation-induced apoptosis in Raji cells. Toxicol Lett 2012; 209: 221-226.
[12] Liu M, Hansen PE, Wang G, Qiu L, Dong J, Yin H, Qian Z, Yang M and Miao J. Pharmacological profile of xanthohumol, a prenylated flavonoid from hops (Humulus lupulus). Molecules 2015; 20: 754-779.
[13] Krajka-Kuzniak V, Paluszczak J and Baer-Dubowska W. Xanthohumol induces phase II enzymes via Nrf2 in human hepatocytes in vitro. Toxicol In Vitro 2013; 27: 149-156.
[14] Szliszka E, Czuba ZP, Mazur B, Sedek L, Paradysz A and Krol W. Chalcones enhance TRAIL-induced apoptosis in prostate cancer cells. Int J Mol Sci 2009; 11: 1-13.
[15] Vene R, Benelli R, Minghelli S, Astigiano S, Tosetti F and Ferrari N. Xanthohumol impairs human prostate cancer cell growth and invasion and diminishes the incidence and progression of advanced tumors in TRAMP mice. Mol Med 2012; 18: 1292-1302.
[16] Herrero AB, San Miguel J and Gutierrez NC. Deregulation of DNA double-strand break repair in multiple myeloma: implications for genome stability. PLoS One 2015; 10: e0121581.
[17] Mustonen R, Bouvier G, Wolber G, Stohr M, Peschke P and Bartsch H. A comparison of gamma and neutron irradiation on Raji cells: effects on DNA damage, repair, cell cycle distribution and lethality. Mutat Res 1999; 429: 169-179.
[18] Drenzek JG, Seiler NL, Jaskula-Sztul R, Rausch MM and Rose SL. Xanthohumol decreases Notch1 expression and cell growth by cell cycle arrest and induction of apoptosis in epithelial ovarian cancer cell lines. Gynecol Oncol 2011; 122: 396-401.
[19] Wang GW, Lv C, Shi ZR, Zeng RT, Dong XY, Zhang WD, Liu RH, Shan L and Shen YH. Abieslactone induces cell cycle arrest and apoptosis in human hepatocellular carcinomas through the mitochondrial pathway and the generation of reactive oxygen species. PLoS One 2014; 9: e115151.
[20] Hall M and Peters G. Genetic alterations of cyclins, cyclin-dependent kinases, and Cdk inhibitors in human cancer. Adv Cancer Res 1996; 68: 67-108.
[21] Deep G and Agarwal R. New combination therapies with cell-cycle agents. Curr Opin Investig Drugs 2008; 9: 591-604.
[22] Lossaint G, Besnard E, Fisher D, Piette J and Dulic V. Chk1 is dispensable for G2 arrest in response to sustained DNA damage when the ATM/p53/p21 pathway is functional. Oncogene 2011; 30: 4261-4274.
[23] Macleod KF, Sherry N, Hannon G, Beach D, Tokino T, Kinzler K, Vogelstein B and Jacks T. p53-dependent and independent expression of p21 during cell growth, differentiation, and DNA damage. Genes Dev 1995; 9: 935-944.
[24] Chaudhary P, Sharma R, Sahu M, Vishwanatha JK, Awasthi S and Awasthi YC. 4-Hydroxynonenal induces G2/M phase cell cycle arrest by activation of the ataxia telangiectasia mutated and Rad3-related protein (ATR)/checkpoint kinase 1 (Chk1) signaling pathway. J Biol Chem 2013; 288: 20532-20546.
[25] Farrell PJ, Allan GJ, Shanahan F, Vousden KH and Crook T. p53 is frequently mutated in Burkitt's lymphoma cell lines. EMBO J 1991; 10: 2879-2887.
[26] Genov M, Kreiseder B, Nagl M, Drucker E, Wiederstein M, Muellauer B, Krebs J, Grohmann T, Pretsch D, Baumann K, Bacher M, Pretsch A and Wiesner C. Tetrahydroanthraquinone derivative (+/-)-4-deoxyaustrocortilutein induces cell cycle arrest and apoptosis in melanoma cells via upregulation of p21 and p53 and downregulation of NF-kappaB. J Cancer 2016; 7: 555-568.
[27] Turinetto V, Porcedda P, Orlando L, De Marchi M, Amoroso A and Giachino C. The cyclin-dependent kinase inhibitor 5, 6-dichloro-1-beta-D-ribofuranosylbenzimidazole induces non-genotoxic, DNA replication-independent apoptosis of normal and leukemic cells, regardless of their p53 status. BMC Cancer 2009; 9: 281.
[28] Giordano A, Whyte P, Harlow E, Franza BR Jr, Beach D and Draetta G. A 60 kd cdc2-associated polypeptide complexes with the E1A proteins in adenovirus-infected cells. Cell 1989; 58: 981-990.

[29] Mukherjee JJ and Kumar S. DNA synthesis inhibition in response to benzo[a]pyrene dihydrodiol epoxide is associated with attenuation of p(34)cdc2: role of p53. Mutat Res 2013; 755: 61-67.

[30] Takase K, Terada N, Szepesi A, Teraoka H, Gelfand EW and Lucas JJ. Release from G0/G1 arrest induced by dimethyl sulfoxide in human lymphoid cells: regulation of synthesis and activation of the p33cdk2 and p34cdc2 kinases. Cell Growth Differ 1994; 5: 1051-1059.

[31] Zhong ZF, Tan W, Wang SP, Qiang WA and Wang YT. Anti-proliferative activity and cell cycle arrest induced by evodiamine on paclitaxel-sensitive and -resistant human ovarian cancer cells. Sci Rep 2015; 5: 16415.

[32] Zhou B, Bu G, Zhou Y, Zhao Y, Li W and Li M. Knockdown of CDC2 expression inhibits proliferation, enhances apoptosis, and increases chemosensitivity to temozolomide in glioblastoma cells. Med Oncol 2015; 32: 378.